Search for $e^+e^- \to K^+K^-\psi(3770)$ at center-of-mass energies from 4.84 to 4.95 GeV

M. Ablikim *et al.*[*]

(BESIII Collaboration)

Using e^+e^- collision data, corresponding to an integrated luminosity of 892 pb^{-1} collected at center-of-mass energies from 4.84 to 4.95 GeV with the BESIII detector, we search for the process $e^+e^- \to K^+K^-\psi(3770)$ by reconstructing two charged kaons and one D meson from $\psi(3770)$. No significant signal of $e^+e^- \to K^+K^-\psi(3770)$ is found and the upper limits of the Born cross sections are reported at 90% confidence level.

I. INTRODUCTION

The charmonium states ($c\bar{c}$) provide an excellent experimental laboratory for understanding the nonperturbative mechanism of quantum chromodynamics (QCD). The conventional charmonium states, like J/ψ, $\psi(2S)$, and $\psi(3770)$, have played a significant role in studying the behavior of quarks and gluons. In recent years, more vector states have been observed in the charmonium energy region, which challenges the conventional charmonium states predicted by the quark potential model [1]. Some of them, such as $\psi(4040)$, $\psi(4160)$ and $\psi(4415)$, have been observed by analyzing the line shape of the cross sections of electron-positron annihilating into inclusive hadron states [2] that are dominated by open-charm processes; others, such as $Y(4230)$, $Y(4390)$, and $Y(4660)$, have been discovered via hidden-charm final states [3–6]. According to the quark potential model [7], the masses of the 5S and 6S vector charmonium states are around 4.6 GeV and 5.2 GeV, respectively. In the mass region of 4.7 GeV to 4.95 GeV, there should be only one vector charmonium 4^3D_1 state with mass about 4.8 GeV. For the exotic states, there are different theoretical predictions based on various hypotheses. For example, in Ref. [8], a vector $\Xi_c\bar{\Xi}_c$ molecule is predicted, whereas lattice QCD does not expect such a state [9]. To resolve this controversial situation, further experimental and theoretical investigations are required.

Recently, BESIII reported a new structure around 4.79 GeV in the line shape of the cross sections of the process $e^+e^- \to D_s^{*+}D_s^{*-}$ [10]. This structure appears to be consistent with the structure observed around 4.71 GeV in BESIII's previous measurement of $e^+e^- \to K^+K^-J/\psi$ [11] and is also evident in $e^+e^- \to K_S^0 K_S^0 J/\psi$ [12], considering the large uncertainties of both mass and width. These new observations inspire us to search for a new process $e^+e^- \to K^+K^-\psi(3770)$. The process $e^+e^- \to \pi^+\pi^-\psi(3770)$ has been studied in the BESIII experiment [13–15]. Searching for new high-mass vector states involving both $\psi(3770)$ and kaons would provide valuable information to determine the nature of these new structures. Although there is no definite theoretical prediction for $e^+e^- \to K^+K^-\psi(3770)$ [Ref. [16] only predicts the inclusive width of $Y(4710)$ decays into J/ψ or $\psi(3686)$], a naive presumption suggests that this process would be suppressed in conventional charmonium [17] or $[cs][\bar{c}\,\bar{s}]$ tetraquark assumptions [18], while an enhancement is expected in the $f_0(980)\psi(2S/1D)$ molecule model [19].

In this paper, for the first time we search for the process $e^+e^- \to K^+K^-\psi(3770)$ by using an integrated luminosity of 892 pb^{-1} e^+e^- collision data collected at center-of-mass (CM) energies from 4.84 to 4.95 GeV with the BESIII detector [20]. The CM energy and corresponding luminosities are listed in Table I.

II. BESIII DETECTOR AND MONTE CARLO

The BESIII detector [21] records symmetric e^+e^- collisions provided by the BEPCII storage ring [22] in the center-of-mass energy range from 2.0 to 4.95 GeV, with a peak luminosity of 1×10^{33} cm^{-2} s^{-1} achieved at $\sqrt{s} = 3.77$ GeV. The cylindrical core of the BESIII detector covers 93% of the full solid angle and consists of a helium-based multilayer drift chamber (MDC), a plastic scintillator time-of-flight system (TOF), and a CsI(Tl) electromagnetic calorimeter (EMC), which are all enclosed in a superconducting solenoidal magnet providing a 1.0 T

TABLE I.   Related quantities at each energy point. Here $\sqrt{s}$ is the CM energy, $\mathcal{L}_{\text{int}}$ is the integrated luminosity, N_{sig} is the number of signal events by the best fit, ϵ_{sig} is the efficiency including the BFs of $\psi(3770)$ and $\bar{D}$ decays, $[1 + \delta(s)]$ is the radiative correction factor, $\frac{1}{|1-\Pi|^2}$ is the vacuum polarization, and σ^B is the upper limit of the Born cross section, and N^{upper} is the upper limit of the signal yield after considering systematic uncertainties.

$\sqrt{s}$ (GeV)	$\mathcal{L}_{\text{int}}$ (pb^{-1})	N_{sig}	N^{upper}	ϵ_{sig} (%)	$[1 + \delta(s)]$	$\frac{1}{|1-\Pi|^2}$	σ^B (pb)
4.84	525.16 ± 2.78	$0.00^{+0.56}_{-0.54}$	<4.7	0.487 ± 0.015	0.727	1.056	<1.2
4.91	207.82 ± 1.10	$3.0^{+4.2}_{-5.2}$	<14.6	1.473 ± 0.027	0.757	1.056	<3.0
4.95	159.28 ± 0.84	$0.8^{+6.1}_{-5.0}$	<14.2	1.736 ± 0.028	0.772	1.056	<3.1

magnetic field. The solenoid is supported by an octagonal flux-return yoke with resistive plate counter muon identifier modules interleaved with steel. The charged-particle momentum resolution at 1 GeV is 0.5%, and the specific energy loss (dE/dx) resolution is 6% for the electrons from Bhabha scattering. The EMC measures photon energies with a resolution of 2.5% (5%) at 1 GeV in the barrel (end cap) region. The time resolution of the TOF barrel part is 68 ps, while the end cap TOF system is upgraded in 2015 with multigap resistive plate chamber technology, providing a time resolution of 60 ps [23,24].

Simulated samples produced with a GEANT4-based [25] Monte Carlo (MC) package, which includes the geometric description [26] of the BESIII detector and the detector response, are used to determine the detection efficiency and to estimate backgrounds. The simulation includes the beam energy spread and initial state radiation (ISR) in the e^+e^- annihilations modeled with the generator KKMC [27]. The inclusive MC sample includes the production of open charm processes, the ISR production of vector charmonium(-like) states, and the continuum processes incorporated in KKMC [27]. All particle decays are modeled with EVTGEN [28] using branching fractions either taken from the Particle Data Group [29], when available, or otherwise estimated with LUNDCHARM [30]. Final state radiation (FSR) from charged final state particles is incorporated using the PHOTOS package [31].

III. EVENT SELECTION

The dominant decay channel of $\psi(3770)$ is $\psi(3770) \rightarrow D\bar{D}$. For the signal process $e^+e^- \rightarrow K^+K^-\psi(3770)$, we only reconstruct two charged kaons and one $\bar{D}$ meson, the presence of D mesons is inferred by the recoiling mass of $K^+K^-\bar{D}$. To reconstruct the $\bar{D}$ mesons, we select nine decay modes with large BF and clean backgrounds, including three modes $\bar{D}^0 \rightarrow K^+\pi^-(3.95\%)$, $\bar{D}^0 \rightarrow K^+\pi^-\pi^0(14.40\%)$ and $\bar{D}^0 \rightarrow K^+\pi^+\pi^-\pi^-(8.22\%)$ with a summed up to a total 26.57% [29] branching fraction of $\bar{D}^0$ decays; six modes $D^- \rightarrow K^+\pi^-\pi^-(9.38\%)$, $D^- \rightarrow K^+\pi^-\pi^-\pi^0(6.25\%)$, $D^- \rightarrow K^0_S\pi^-(1.56\%)$, $D^- \rightarrow K^0_S\pi^-\pi^0(7.36\%)$, $D^- \rightarrow K^0_S\pi^-\pi^-\pi^+(3.10\%)$, and $D^- \rightarrow K^+K^-\pi^-(0.97\%)$ with a summed up to 28.62% [29]

branching fraction of D^- decays. Throughout the whole text, charge conjugated decays are always implied.

Charged tracks detected in the MDC are required to be within a polar angle (θ) range of $|\cos\theta| < 0.93$, where θ is defined with respect to the z-axis, which is the symmetry axis of the MDC. For charged tracks not originating from K^0_S decays, the distance of closest approach to the interaction point (IP) must be less than 10 cm along the z-axis, $|V_z|$, and less than 1 cm in the transverse plane, $|V_{xy}|$. Particle identification (PID) for charged tracks combines measurements of the energy deposited in the MDC (dE/dx) and the flight time in the TOF to form likelihoods $\mathcal{L}(h)(h = p, K, \pi)$ for each hadron h hypothesis. Charged kaons and pions are identified by comparing the likelihoods for the kaon and pion hypotheses, $\mathcal{L}(K) > \mathcal{L}(\pi)$ and $\mathcal{L}(\pi) > \mathcal{L}(K)$, respectively.

Each K^0_S candidate is reconstructed from two oppositely charged tracks satisfying $|V_z| < 20$ cm. The two charged tracks are assigned as $\pi^+\pi^-$ without imposing further PID criteria. They are constrained to originate from a common vertex and are required to have an invariant mass within $(0.486, 0.510)$ GeV/c^2. This mass window corresponds to about three times the mass resolution. The decay length of the K^0_S candidate is required to be greater than twice the vertex resolution away from the IP.

The π^0 candidates are reconstructed via $\pi^0 \rightarrow \gamma\gamma$. Here, photon candidates are identified using showers in the EMC. The deposited energy of each shower must be more than 25 MeV in the barrel region $(|\cos\theta| < 0.80)$ and more than 50 MeV in the end cap region $(0.86 < |\cos\theta| < 0.92)$. To exclude showers that originate from charged tracks, the angle subtended by the EMC shower and the position of the closest charged track at the EMC must be greater than 10 degrees as measured from the IP. To suppress electronic noise and showers unrelated to the event, the difference between the EMC time and the event start time is required to be within [0, 700] ns. A one-constraint (1C) kinematic fit is performed to constrain the invariant mass of photon pair to the nominal mass of π^0 [29], and a list of π^0 candidates is prepared for subsequent event selection.

If there are multiple reconstructed $\bar{D}$ candidates, the one with the closest mass to the nominal $\bar{D}$ mass [29] is selected. A 1C kinematic fit is then carried out with the $\bar{D}$
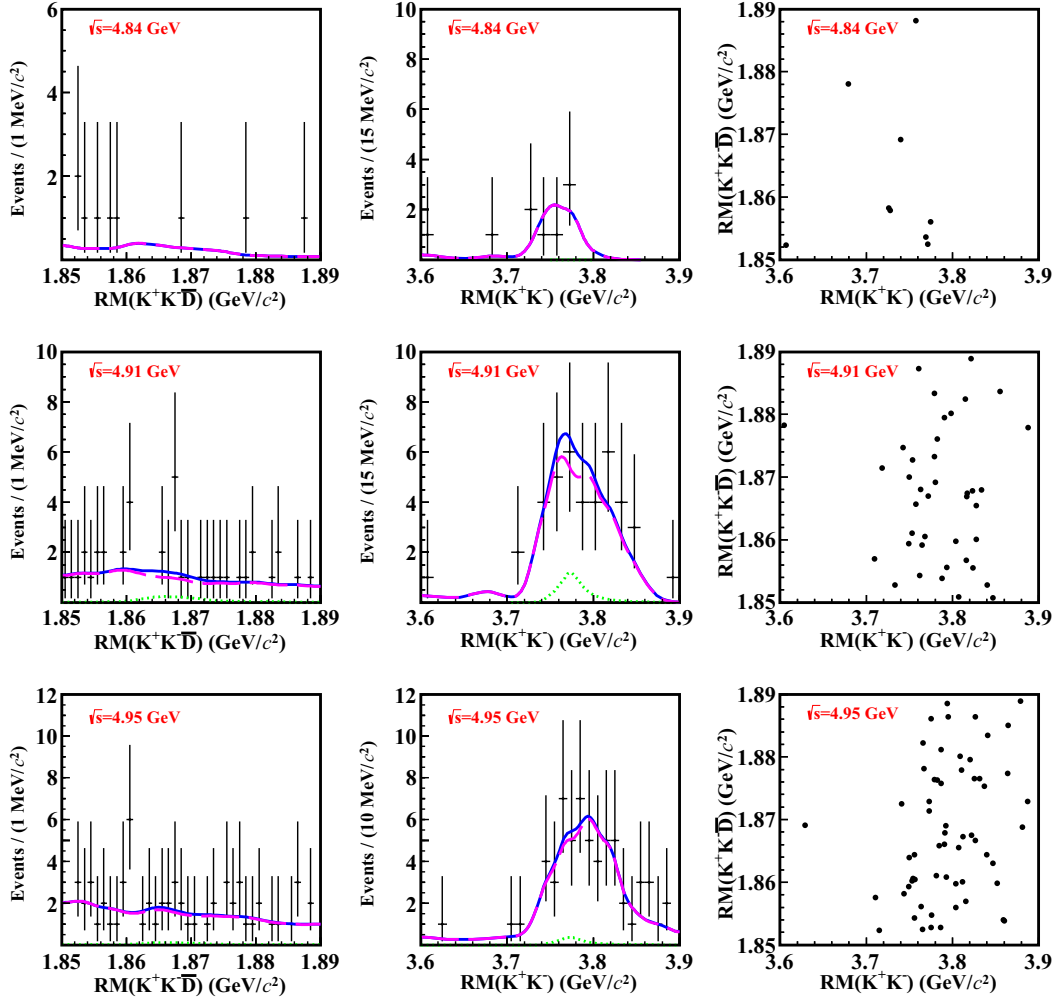
FIG. 1. The recoiling mass distributions of $K^+K^-\bar{D}$ (left panel) and K^+K^- (middle panel), and their 2D scatter plot (right panel) at $\sqrt{s} = 4.84$, 4.91, and 4.95 GeV. In the left two columns, the dots with error bars are data, the blue solid lines represent the fitted curve, the green dotted lines represent signal shapes, the pink dashed lines present backgrounds. Notice at $\sqrt{s} = 4.84$, the signals are too tiny to be visible.

meson's nominal mass constraint to improve the resolution of the recoiling mass spectrum and to reduce the background. The χ^2 value of the 1C kinematic fit is set to be less than 13. This selection criterion is optimized by maximizing the Punzi figure of merit, $\frac{S}{\sqrt{B}+\alpha/2}$ [32], where S is the number of signal from the signal MC sample, B is the estimated background yield from the inclusive MC samples, and α, set at 3, is the expected significance. The $K^{\pm}$ candidates, which meet the particle identification criteria and possess the lowest momentum among those not utilized in $\bar{D}$ reconstruction, are assumed to be the bachelor kaons unrelated to D or $\bar{D}$ decays.

Even though the process $e^+e^- \to \phi\psi(3770)$ is highly suppressed in a electron-positron collision experiment due to C-parity violation, we require the $|M_{K^+K^-} - M_\phi| > 0.02$ GeV/c^2 to reduce the backgrounds including ϕ meson in the final states, in which the $M_{K^+K^-}$ and M_ϕ denote the

invariant mass of K^+K^- and ϕ nominal mass, respectively. After imposing all event selection criteria, we compare the recoiling mass distributions, $R(K^+K^-\bar{D})$ and $R(K^+K^-)$, between data and inclusive MC sample, as shown in Fig. 1. Here, $R(K^+K^-\bar{D}) = \sqrt{(P_{e^+e^-} - P_{K^+} - P_{K^-} - P_{\bar{D}})^2}$ and $R(K^+K^-) = \sqrt{(P_{e^+e^-} - P_{K^+} - P_{K^-})^2}$ are the recoil mass of the $K^+K^-\bar{D}$ and K^+K^-, respectively, where $P_{e^+e^-}$, $P_{K^{\pm}}$ and $P_{\bar{D}}$ are the 4-momenta of the initial e^+e^- system, the $K^{\pm}$ and $\bar{D}$, respectively. In general, the data can be well described by the inclusive MC sample.

IV. DATA ANALYSIS

To extract the signal yields, a two-dimensional (2D) unbinned maximum likelihood fit is performed to the recoiling mass distributions $RM(K^+K^-\bar{D})$ versus $RM(K^+K^-)$. The 2D probability density function (PDF) for the signal is taken from the signal MC simulation. The

PDFs of background contributions are extracted from the inclusive MC samples. The dominant backgrounds come from $\pi^+\pi^- D\bar{D}\pi^0$ and $\pi^+\pi^- D\bar{D}\pi^0\pi^0$ processes. Neither unexpected structure nor peaking background is found from the inclusive MC in the fitting region. To further test the reliability of background shape, we compare the $RM(K^+K^-\bar{D})$ and $RM(K^+K^-)$ distributions (include signal region and nonsignal region) between data and MC simulation without any requirement on the χ^2 of D kinematic fit. No significant difference between data and inclusive MC sample is found. Since no significant signal of $e^+e^- \rightarrow K^+K^-D\bar{D}$ is observed and the $D\bar{D}$ invariant mass distribution of $e^+e^- \rightarrow K^+K^-D\bar{D}$ is similar with that of $\psi(3770)$ because of the limited phase space, this component is ignored in the fits. Figure 1 shows the $RM(K^+K^-\bar{D})$ versus $RM(K^+K^-)$ fitting results at CM energies $\sqrt{s} = 4.84, 4.91,$ and 4.95 GeV.

In the fits at each energy points, the cross sections of $e^+e^- \rightarrow K^+K^-\psi(3770)$ with $\psi(3770) \rightarrow D^0\bar{D}^0$ and $\psi(3770) \rightarrow D^+D^-$ are constrained to be the same. Therefore, after considering the detection efficiency and BF of $\bar{D}$ decays, the ratios of the signal yields in the charged mode relative to the neutral modes are fixed to $f_{4.84} = 0.46$, $f_{4.91} = 0.53$, and $f_{4.95} = 0.54$ for the three energy points, respectively.

The Born cross section is calculated as,

$$\sigma^B(e^+e^- \rightarrow K^+K^-\psi(3770))$$
$$= \frac{N_{\text{sig}}}{2\mathcal{L}_{\text{int}}(1 + \delta(s))\frac{1}{|1-\Pi|^2}\epsilon_{\text{sig}}B_{\text{sub}}}, \quad (1)$$

where N_{sig} is the number of signal events in the data, $\mathcal{L}_{\text{int}}$ is the integrated luminosity of data measured by Bhabha events [20], ϵ_{sig} is the detection efficiency, B_{sub} is aggregate of the BFs of $\psi(3770) \rightarrow D\bar{D}$ and subsequent D decays across the nine tag modes, $\frac{1}{|1-\Pi|^2}$ is the vacuum polarization factor [33], and $1 + \delta(s)$ is the radiative correction factor defined as

$$1 + \delta(s) = \frac{\int \sigma(s(1-x))F(x,s)dx}{\sigma(s)}, \quad (2)$$

where $F(x,s)$ is radiator function calculated by QED with accuracy 0.1% [34]. σ is the cross section.

No obvious signal is found for the process $e^+e^- \rightarrow K^+K^-\psi(3770)$. Utilizing the Bayesian approach [35] and incorporating the systematic uncertainties, that will be discussed in Sec. IV, we estimate the upper limits on the Born cross sections for $e^+e^- \rightarrow K^+K^-\psi(3770)$ at 90% confidence level at these three energy points. The corresponding likelihood distributions are shown in Fig. 2, and the upper limit results are listed in Table I.
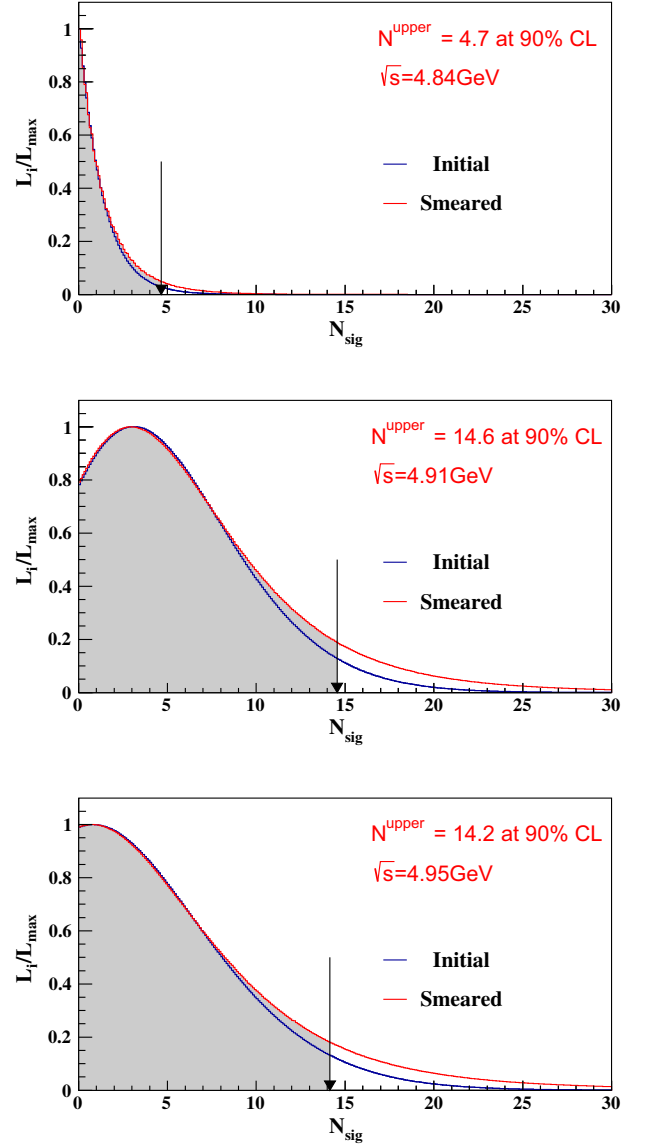

FIG. 2. Normalized likelihood (L/L_{max}) as a function of the number of signal events. The red and blue solid curves are the likelihood distributions before and after involving the multiplicative systematic uncertainties, respectively. The black arrow shows the upper limit of the number of events at 90% confidence level after considering the systematic uncertainties.

V. SYSTEMATIC UNCERTAINTY

In the measurements of the Born cross sections, the systematic uncertainties are categorized into additive and multiplicative uncertainties. The additive uncertainties originate from the fit to the $RM(K^+K^-\bar{D})$ versus $RM(K^+K^-)$, that directly affects the fitting results. The multiplicative uncertainties are associated with the efficiencies, and will affect the cross section calculation.

The additive uncertainties originate from the 2D fits, which are primarily influenced by the uncertainty in the signal and background shapes. The uncertainty associated

with the signal shape is negligible. In the nominal determination of the upper limits, the background shape is derived from the inclusive MC simulation. To assess the corresponding systematic uncertainty, a 2D polynomial function is utilized as an alternate option. The 2D polynomial function is formed by the product of two polynomial functions corresponding to $RM(K^+K^-\bar{D})$ and $RM(K^+K^-)$. For the $RM(K^+K^-\bar{D})$ dimension, we have experimented with a constant and a 1st-order polynomial function, whereas for the $RM(K^+K^-)$ dimension, we have explored 2nd and 3rd-order polynomial functions. The resulting upper limits based on these two background shapes are detailed in Table I, and the larger values are selected for conservation.

The multiplicative uncertainties include luminosity ($\mathcal{L}_{\text{int}}$), $K^\pm$ and $\pi^\pm$ tracking and PID, π^0 reconstruction, radiative correction factor $[1 + \delta(s)]$, K_S^0 reconstruction, 1C kinematic fit, MC statistics, and quoted BFs. The integrated luminosity is measured using Bhabha events, the uncertainty is about 0.6% [20]. The $K^\pm$ tracking and PID efficiencies are estimated by double tag hadronic $D\bar{D}$ events [36]. The data/MC efficiency differences are weighted by the corresponding momentum spectra from signal MC events. The $K^\pm$ tracking and PID systematic uncertainties are determined to be 8.5% and 2.9%, respectively. The systematic uncertainties of $\pi^\pm$ tracking and PID are cited from previous work, the systematic uncertainty is 1.6% for both tracking and PID [37]. In this work, the π^0 selection criteria are the same as those used in Ref. [38]. We assign 1.0% as the systematic uncertainty per π^0 reconstruction, which includes the effect of photon selection, mass window and 1C kinematic fit. The systematic uncertainty of radiative correction factor is estimated by comparing the difference between factors obtained by the phase space line shape and flat line shape, and is determined to be 10.0%, 10.5%, and 11.0% for $\sqrt{s} = 4.84, 4.91$, and 4.95 GeV, respectively. The systematic uncertainty of quoted BFs is 10%, including the $\psi(3770) \rightarrow D\bar{D}$ and $\bar{D}$ subsequent decays [29]. The systematic uncertainty of K_S^0 reconstruction is 0.2%, quoting from Ref. [36]. For the uncertainty of kinematic fit, we try to correct the track helix parameters in the MC simulation so as to describe the data better. The correction factors are obtained by using control sample $J/\psi \rightarrow \phi f_0(980)$ [39]. The efficiency difference before and after the correction, 1%, is taken as the systematic uncertainty of the kinematic fit. The uncertainties of MC statistics are 3.1%, 1.8%, and 1.6% for $\sqrt{s} = 4.84, 4.91$, and 4.95 GeV, respectively. The uncertainties associated with the physics model are estimated by comparing the detection efficiencies with those of phase space and $e^+e^- \rightarrow f_0(980)\psi(3770) \rightarrow K^+K^-\psi(3770)$. The relative differences, which are 15.6%, 17.6%, and 20.0% for $\sqrt{s} = 4.84, 4.91$, and 4.95 GeV, respectively, are reported as the corresponding systematic uncertainties. Adding each systematic uncertainty in quadrature, we

TABLE II. Multiplicative systematic uncertainties (%) in the measurements of the Born cross sections.

Uncertainty	4.84 GeV	4.91 GeV	4.95 GeV
Luminosity	0.6	0.6	0.6
$K^\pm$ tracking	8.5	8.5	8.5
$K^\pm$ PID	2.9	2.9	2.9
$\pi^\pm$ tracking	1.6	1.6	1.6
$\pi^\pm$ PID	1.6	1.6	1.6
Radiative correction factor	10.0	10.5	11.0
Quoted $\mathcal{B}$	10.0	10.0	10.0
K_S^0 reconstruction	0.2	0.2	0.2
Kinematic fit	1.0	1.0	1.0
MC statistics	3.1	1.8	1.6
Physics model	15.6	17.6	20.0
Total	23.2	24.7	26.7

obtain the total systematic uncertainties for each energy point. All the multiplicative systematic uncertainties are summarized in Table II. The blue and red lines in Fig. 2 show with and without considering the systematic uncertainty likelihood distribution.

VI. SUMMARY

In this paper, we search for the process $e^+e^- \rightarrow K^+K^-\psi(3770)$ using 896 pb^{-1} of e^+e^- annihilation data taken at CM energies from 4.84 to 4.95 GeV. No significant signal for $e^+e^- \rightarrow K^+K^-\psi(3770)$ is observed. Therefore, we determine the upper limits of the Born cross sections at 90% confidence level to be 1–3 pb. We also notice that the upper limits reported in this paper are obviously smaller than the cross sections measured in the process $e^+e^- \rightarrow \pi^+\pi^-D^+D^-$ [15], which could be attributed to a combination of factors, including the suppressed phase space and strange quark production in $e^+e^- \rightarrow K^+K^-\psi(3770)$. But we do not know which factor is dominant at present. Further measurements based on additional data samples within and beyond this energy region, that will be collected at BESIII in the future, may help to clarify this matter.

[1] S. Godfrey and N. Isgur, Phys. Rev. D **32**, 189 (1985).

[2] M. Ablikim *et al.* (BES Collaboration), Phys. Lett. B **660**, 315 (2008).

[3] B. Aubert *et al.* (*BABAR* Collaboration), Phys. Rev. Lett. **95**, 142001 (2005).

[4] B. Aubert *et al.* (*BABAR* Collaboration), Phys. Rev. Lett. **98**, 212001 (2007).

[5] M. Ablikim *et al.* (BESIII Collaboration), Phys. Rev. D **104**, 052012 (2021).

[6] G. Pakhlova *et al.* (Belle Collaboration), Phys. Rev. Lett. **101**, 172001 (2008).

[7] V. Kher and A. K. Rai, Chin. Phys. C **42**, 083101 (2018).

[8] X. K. Dong, F. K. Guo, and B. S. Zou, Prog. Phys. **41**, 65 (2021).

[9] T. W. Chiu *et al.* (TWQCD Collaboration), Phys. Rev. D **73**, 094510 (2006).

[10] M. Ablikim *et al.* (BESIII Collaboration), Phys. Rev. Lett. **131**, 151903 (2023).

[11] M. Ablikim *et al.* (BESIII Collaboration), Phys. Rev. Lett. **131**, 211902 (2023).

[12] M. Ablikim *et al.* (BESIII Collaboration), Phys. Rev. D **107**, 092005 (2023).

[13] M. Ablikim *et al.* (BESIII Collaboration), Phys. Rev. D **100**, 032005 (2019).

[14] M. Ablikim *et al.* (BESIII Collaboration), Phys. Lett. B **804**, 135395 (2020).

[15] M. Ablikim *et al.* (BESIII Collaboration), Phys. Rev. D **106**, 052012 (2022).

[16] N. Brambilla, W. K. Lai, A. Mohapatra, and A. Vairo, Phys. Rev. D **107**, 054034 (2023).

[17] R. Q. Qian and X. Liu, Phys. Rev. D **108**, 094046 (2023).

[18] Q. F. Lü and Y. B. Dong, Phys. Rev. D **94**, 074007 (2016).

[19] F. K. Guo, C. Hanhart, and U. G. Meissner, Phys. Lett. B **665**, 26 (2008).

[20] M. Ablikim *et al.* (BESIII Collaboration), Chin. Phys. C **46**, 113003 (2022).

[21] M. Ablikim *et al.* (BESIII Collaboration), Nucl. Instrum. Methods Phys. Res., Sect. A **614**, 345 (2010).

[22] C. H. Yu *et al.*, *Proceedings of IPAC2016, Busan, Korea* (2016), 10.18429/JACoW-IPAC2016-TUYA01.

[23] X. Li *et al.*, Radiat. Detect. Technol. Methods **1**, 13 (2017).

[24] Y. X. Guo *et al.*, Radiat. Detect. Technol. Methods **1**, 15 (2017).

[25] S. Agostinelli *et al.* (GEANT4 Collaboration), Nucl. Instrum. Methods Phys. Res., Sect. A **506**, 250 (2003).

[26] K. X. Huang *et al.*, Nucl. Sci. Tech. **33**, 142 (2022).

[27] S. Jadach, B. F. L. Ward, and Z. Was, Phys. Rev. D **63**, 113009 (2001); Comput. Phys. Commun. **130**, 260 (2000).

[28] D. J. Lange, Nucl. Instrum. Methods Phys. Res., Sect. A **462**, 152 (2001); R. G. Ping, Chin. Phys. C **32**, 599 (2008).

[29] R. L. Workman *et al.* (Particle Data Group), Prog. Theor. Exp. Phys. **2022**, 083C01 (2022).

[30] J. C. Chen, G. S. Huang, X. R. Qi, D. H. Zhang, and Y. S. Zhu, Phys. Rev. D **62**, 034003 (2000).

[31] E. Richter-Was, Phys. Lett. B **303**, 163 (1993).

[32] Giovanni Punzi, eConf C **030908**, MODT002 (2003), https://www.slac.stanford.edu/econf/C030908/papers/MODT002.pdf.

[33] S. Actis *et al.* (Working Group on Radiative Corrections and Monte Carlo Generators for Low Energies Collaboration), Eur. Phys. J. C **66**, 585 (2010).

[34] E. A. Kuraev and V. S. Fadin, Sov. J. Nucl. Phys. **41**, 466 (1985), https://api.semanticscholar.org/CorpusID:124372625.

[35] K. Stenson, arXiv:physics/0605236.

[36] M. Ablikim *et al.* (BESIII Collaboration), Phys. Rev. D **104**, 052008 (2021).

[37] M. Ablikim *et al.* (BESIII Collaboration), Phys. Rev. D **97**, 072004 (2018).

[38] M. Ablikim *et al.* (BESIII Collaboration), Eur. Phys. J. C **76,** 369 (2016).

[39] M. Ablikim *et al.* (BESIII Collaboration), Phys. Rev. D **87,** 012002 (2013).

M. Ablikim,[1] M. N. Achasov,[4,b] P. Adlarson,[75] O. Afedulidis,[3] X. C. Ai,[80] R. Aliberti,[35] A. Amoroso,[74a,74c] Q. An,[71,58] Y. Bai,[57] O. Bakina,[36] I. Balossino,[29a] Y. Ban,[46,g] H.-R. Bao,[63] V. Batozskaya,[1,44] K. Begzsuren,[32] N. Berger,[35] M. Berlowski,[44] M. Bertani,[28a] D. Bettoni,[29a] F. Bianchi,[74a,74c] E. Bianco,[74a,74c] A. Bortone,[74a,74c] I. Boyko,[36] R. A. Briere,[5] A. Brueggemann,[68] H. Cai,[76] X. Cai,[1,58] A. Calcaterra,[28a] G. F. Cao,[1,63] N. Cao,[1,63] S. A. Cetin,[62a] J. F. Chang,[1,58] W. L. Chang,[1,63] G. R. Che,[43] G. Chelkov,[36,a] C. Chen,[43] C. H. Chen,[9] Chao Chen,[55] G. Chen,[1] H. S. Chen,[1,63] M. L. Chen,[1,58,63] S. J. Chen,[42] S. L. Chen,[45] S. M. Chen,[61] T. Chen,[1,63] X. R. Chen,[31,63] X. T. Chen,[1,63] Y. B. Chen,[1,58] Y. Q. Chen,[34] Z. J. Chen,[25,h] Z. Y. Chen,[1,63] S. K. Choi,[10] X. Chu,[43] G. Cibinetto,[29a] F. Cossio,[74c] J. J. Cui,[50] H. L. Dai,[1,58] J. P. Dai,[78] A. Dbeyssi,[18] R. E. de Boer,[3] D. Dedovich,[36] C. Q. Deng,[72] Z. Y. Deng,[1] A. Denig,[35] I. Denysenko,[36] M. Destefanis,[74a,74c] F. De Mori,[74a,74c] B. Ding,[66,1] X. X. Ding,[46,g] Y. Ding,[34] Y. Ding,[40] J. Dong,[1,58] L. Y. Dong,[1,63] M. Y. Dong,[1,58,63] X. Dong,[76] M. C. Du,[1] S. X. Du,[80] Z. H. Duan,[42] P. Egorov,[36,a] Y. H. Fan,[45] J. Fang,[1,58] J. Fang,[59] S. S. Fang,[1,63] W. X. Fang,[1] Y. Fang,[1] Y. Q. Fang,[1,58] R. Farinelli,[29a] L. Fava,[74b,74c] F. Feldbauer,[3] G. Felici,[28a] C. Q. Feng,[71,58] J. H. Feng,[59] Y. T. Feng,[71,58] K. Fischer,[69] M. Fritsch,[3] C. D. Fu,[1] J. L. Fu,[63] Y. W. Fu,[1] H. Gao,[63] Y. N. Gao,[46,g] Yang Gao,[71,58] S. Garbolino,[74c] I. Garzia,[29a,29b] L. Ge,[80] P. T. Ge,[76] Z. W. Ge,[42] C. Geng,[59] E. M. Gersabeck,[67] A. Gilman,[69] K. Goetzen,[13] L. Gong,[40] W. X. Gong,[1,58] W. Gradl,[35] S. Gramigna,[29a,29b] M. Greco,[74a,74c] M. H. Gu,[1,58] Y. T. Gu,[15] C. Y. Guan,[1,63] Z. L. Guan,[22] A. Q. Guo,[31,63] L. B. Guo,[41] M. J. Guo,[50] R. P. Guo,[49] Y. P. Guo,[12,f] A. Guskov,[36,a] J. Gutierrez,[27] K. L. Han,[63] T. T. Han,[1] X. Q. Hao,[19] F. A. Harris,[65] K. K. He,[55] K. L. He,[1,63] F. H. Heinsius,[3] C. H. Heinz,[35] Y. K. Heng,[1,58,63] C. Herold,[60] T. Holtmann,[3] P. C. Hong,[12,f] G. Y. Hou,[1,63] X. T. Hou,[1,63] Y. R. Hou,[63] Z. L. Hou,[1] B. Y. Hu,[59] H. M. Hu,[1,63] J. F. Hu,[56,i] T. Hu,[1,58,63] Y. Hu,[1] G. S. Huang,[71,58] K. X. Huang,[59] L. Q. Huang,[31,63] X. T. Huang,[50] Y. P. Huang,[1] T. Hussain,[73] F. Hölzken,[3] N. Hüsken,[27,35] N. in der Wiesche,[68] M. Irshad,[71,58] J. Jackson,[27] S. Janchiv,[32] J. H. Jeong,[10] Q. Ji,[1] Q. P. Ji,[19] W. Ji,[1,63] X. B. Ji,[1,63] X. L. Ji,[1,58] Y. Y. Ji,[50] X. Q. Jia,[50] Z. K. Jia,[71,58] D. Jiang,[1,63] H. B. Jiang,[76] P. C. Jiang,[46,g] S. S. Jiang,[39] T. J. Jiang,[16] X. S. Jiang,[1,58,63] Y. Jiang,[63] J. B. Jiao,[50] J. K. Jiao,[34] Z. Jiao,[23] S. Jin,[42] Y. Jin,[66] M. Q. Jing,[1,63] X. M. Jing,[63] T. Johansson,[75] S. Kabana,[33] N. Kalantar-Nayestanaki,[64] X. L. Kang,[9] X. S. Kang,[40] M. Kavatsyuk,[64] B. C. Ke,[80] V. Khachatryan,[27] A. Khoukaz,[68] R. Kiuchi,[1] O. B. Kolcu,[62a] B. Kopf,[3] M. Kuessner,[3] X. Kui,[1,63] N. Kumar,[26] A. Kupsc,[44,75] W. Kühn,[37] J. J. Lane,[67] P. Larin,[18] L. Lavezzi,[74a,74c] T. T. Lei,[71,58] Z. H. Lei,[71,58] H. Leithoff,[35] M. Lellmann,[35] T. Lenz,[35] C. Li,[47] C. Li,[43] C. H. Li,[39] Cheng Li,[71,58] D. M. Li,[80] F. Li,[1,58] G. Li,[1] H. Li,[71,58] H. B. Li,[1,63] H. J. Li,[19] H. N. Li,[56,i] Hui Li,[43] J. R. Li,[61] J. S. Li,[59] Ke Li,[1] L. J. Li,[1,63] L. K. Li,[1] Lei Li,[48] M. H. Li,[43] P. R. Li,[38,k] Q. M. Li,[1,63] Q. X. Li,[50] R. Li,[17,31] S. X. Li,[12] T. Li,[50] W. D. Li,[1,63] W. G. Li,[1] X. Li,[1,63] X. H. Li,[71,58] X. L. Li,[50] Xiaoyu Li,[1,63] Y. G. Li,[46,g] Z. J. Li,[59] Z. X. Li,[15] C. Liang,[42] H. Liang,[71,58] H. Liang,[1,63] Y. F. Liang,[54] Y. T. Liang,[31,63] G. R. Liao,[14] L. Z. Liao,[50] Y. P. Liao,[1,63] J. Libby,[26] A. Limphirat,[60] D. X. Lin,[31,63] T. Lin,[1] B. J. Liu,[1] B. X. Liu,[76] C. Liu,[34] C. X. Liu,[1] F. H. Liu,[53] Fang Liu,[1] Feng Liu,[6] G. M. Liu,[56,i] H. Liu,[38,j,k] H. B. Liu,[15] H. M. Liu,[1,63] Huanhuan Liu,[1] Huihui Liu,[21] J. B. Liu,[71,58] J. Y. Liu,[1,63] K. Liu,[38,j,k] K. Y. Liu,[40] Ke Liu,[22] L. Liu,[71,58] L. C. Liu,[43] Lu Liu,[43] M. H. Liu,[12,f] P. L. Liu,[1] Q. Liu,[63] S. B. Liu,[71,58] T. Liu,[12,f] W. K. Liu,[43] W. M. Liu,[71,58] X. Liu,[38,j,k] X. Liu,[39] Y. Liu,[38,j,k] Y. Liu,[80] Y. B. Liu,[43] Z. A. Liu,[1,58,63] Z. D. Liu,[9] Z. Q. Liu,[50] X. C. Lou,[1,58,63] F. X. Lu,[59] H. J. Lu,[23] J. G. Lu,[1,58] X. L. Lu,[1] Y. Lu,[7] Y. P. Lu,[1,58] Z. H. Lu,[1,63] C. L. Luo,[41] M. X. Luo,[79] T. Luo,[12,f] X. L. Luo,[1,58] X. R. Lyu,[63] Y. F. Lyu,[43] F. C. Ma,[40] H. Ma,[78] H. L. Ma,[1] J. L. Ma,[1,63] L. L. Ma,[50] M. M. Ma,[1,63] Q. M. Ma,[1] R. Q. Ma,[1,63] X. T. Ma,[1,63] X. Y. Ma,[1,58] Y. Ma,[46,g] Y. M. Ma,[31] F. E. Maas,[18] M. Maggiora,[74a,74c] S. Malde,[69] A. Mangoni,[28b] Y. J. Mao,[46,g] Z. P. Mao,[1] S. Marcello,[74a,74c] Z. X. Meng,[66] J. G. Messchendorp,[13,64] G. Mezzadri,[29a] H. Miao,[1,63] T. J. Min,[42] R. E. Mitchell,[27] X. H. Mo,[1,58,63] B. Moses,[27] N. Yu. Muchnoi,[4,b] J. Muskalla,[35] Y. Nefedov,[36] F. Nerling,[18,d] I. B. Nikolaev,[4,b] Z. Ning,[1,58] S. Nisar,[11,l] Q. L. Niu,[38,j,k] W. D. Niu,[55] Y. Niu,[50] S. L. Olsen,[63] Q. Ouyang,[1,58,63] S. Pacetti,[28b,28c] X. Pan,[55] Y. Pan,[57] A. Pathak,[34] P. Patteri,[28a] Y. P. Pei,[71,58] M. Pelizaeus,[3] H. P. Peng,[71,58] Y. Y. Peng,[38,j,k] K. Peters,[13,d] J. L. Ping,[41] R. G. Ping,[1,63] S. Plura,[35] V. Prasad,[33] F. Z. Qi,[1] H. Qi,[71,58] H. R. Qi,[61] M. Qi,[42] T. Y. Qi,[12,f] S. Qian,[1,58] W. B. Qian,[63] C. F. Qiao,[63] X. K. Qiao,[80] J. J. Qin,[72] L. Q. Qin,[14] X. S. Qin,[50] Z. H. Qin,[1,58] J. F. Qiu,[1] S. Q. Qu,[61] Z. H. Qu,[72] C. F. Redmer,[35] K. J. Ren,[39] A. Rivetti,[74c] M. Rolo,[74c] G. Rong,[1,63] Ch. Rosner,[18] S. N. Ruan,[43] N. Salone,[44] A. Sarantsev,[36,c] Y. Schelhaas,[35] K. Schoenning,[75] M. Scodeggio,[29a] K. Y. Shan,[12,f] W. Shan,[24] X. Y. Shan,[71,58] Z. J. Shang,[38,j,k] J. F. Shangguan,[16] L. G. Shao,[1,63] M. Shao,[71,58]

C. P. Shen,[12,f] H. F. Shen,[1,8] W. H. Shen,[63] X. Y. Shen,[1,63] B. A. Shi,[63] H. C. Shi,[71,58] J. L. Shi,[12] J. Y. Shi,[1] Q. Q. Shi,[55] R. S. Shi,[1,63] S. Y. Shi,[72] X. Shi,[1,58] J. J. Song,[19] T. Z. Song,[59] W. M. Song,[34,1] Y. J. Song,[12] Y. X. Song,[46,g,m] S. Sosio,[74a,74c] S. Spataro,[74a,74c] F. Stieler,[35] Y. J. Su,[63] G. B. Sun,[76] G. X. Sun,[1] H. Sun,[63] H. K. Sun,[1] J. F. Sun,[19] K. Sun,[61] L. Sun,[76] S. S. Sun,[1,63] T. Sun,[51,e] W. Y. Sun,[34] Y. Sun,[9] Y. J. Sun,[71,58] Y. Z. Sun,[1] Z. Q. Sun,[1,63] Z. T. Sun,[50] C. J. Tang,[54] G. Y. Tang,[1] J. Tang,[59] Y. A. Tang,[76] L. Y. Tao,[72] Q. T. Tao,[25,h] M. Tat,[69] J. X. Teng,[71,58] V. Thoren,[75] W. H. Tian,[59] Y. Tian,[31,63] Z. F. Tian,[76] I. Uman,[62b] Y. Wan,[55] S. J. Wang,[50] B. Wang,[1] B. L. Wang,[63] Bo Wang,[71,58] D. Y. Wang,[46,g] F. Wang,[72] H. J. Wang,[38,j,k] J. P. Wang,[50] K. Wang,[1,58] L. L. Wang,[1] M. Wang,[50] Meng Wang,[1,63] N. Y. Wang,[63] S. Wang,[38,j,k] S. Wang,[12,f] T. Wang,[12,f] T. J. Wang,[43] W. Wang,[59] W. Wang,[72] W. P. Wang,[71,58] X. Wang,[46,g] X. F. Wang,[38,j,k] X. J. Wang,[39] X. L. Wang,[12,f] X. N. Wang,[1] Y. Wang,[61] Y. D. Wang,[45] Y. F. Wang,[1,58,63] Y. L. Wang,[19] Y. N. Wang,[45] Y. Q. Wang,[1] Yaqian Wang,[17] Yi Wang,[61] Z. Wang,[1,58] Z. L. Wang,[72] Z. Y. Wang,[1,63] Ziyi Wang,[63] D. Wei,[70] D. H. Wei,[14] F. Weidner,[68] S. P. Wen,[1] Y. R. Wen,[39] U. Wiedner,[3] G. Wilkinson,[69] M. Wolke,[75] L. Wollenberg,[3] C. Wu,[39] J. F. Wu,[1,8] L. H. Wu,[1] L. J. Wu,[1,63] X. Wu,[12,f] X. H. Wu,[34] Y. Wu,[71] Y. H. Wu,[55] Y. J. Wu,[31] Z. Wu,[1,58] L. Xia,[71,58] X. M. Xian,[39] B. H. Xiang,[1,63] T. Xiang,[46,g] D. Xiao,[38,j,k] G. Y. Xiao,[42] S. Y. Xiao,[1] Y. L. Xiao,[12,f] Z. J. Xiao,[41] C. Xie,[42] X. H. Xie,[46,g] Y. Xie,[50] Y. G. Xie,[1,58] Y. H. Xie,[6] Z. P. Xie,[71,58] T. Y. Xing,[1,63] C. F. Xu,[1,63] C. J. Xu,[59] G. F. Xu,[1] H. Y. Xu,[66] Q. J. Xu,[16] Q. N. Xu,[30] W. Xu,[1] W. L. Xu,[66] X. P. Xu,[55] Y. C. Xu,[77] Z. P. Xu,[42] Z. S. Xu,[63] F. Yan,[12,f] L. Yan,[12,f] W. B. Yan,[71,58] W. C. Yan,[80] X. Q. Yan,[1] H. J. Yang,[51,e] H. L. Yang,[34] H. X. Yang,[1] Tao Yang,[1] Y. Yang,[12,f] Y. F. Yang,[43] Y. X. Yang,[1,63] Yifan Yang,[1,63] Z. W. Yang,[38,j,k] Z. P. Yao,[50] M. Ye,[1,58] M. H. Ye,[8] J. H. Yin,[1] Z. Y. You,[59] B. X. Yu,[1,58,63] C. X. Yu,[43] G. Yu,[1,63] J. S. Yu,[25,h] T. Yu,[72] X. D. Yu,[46,g] Y. C. Yu,[80] C. Z. Yuan,[1,63] J. Yuan,[34] L. Yuan,[2] S. C. Yuan,[1] Y. Yuan,[1,63] Z. Y. Yuan,[59] C. X. Yue,[39] A. A. Zafar,[73] F. R. Zeng,[50] S. H. Zeng,[72] X. Zeng,[12,f] Y. Zeng,[25,h] Y. J. Zeng,[59] Y. J. Zeng,[1,63] X. Y. Zhai,[34] Y. C. Zhai,[50] Y. H. Zhan,[59] A. Q. Zhang,[1,63] B. L. Zhang,[1,63] B. X. Zhang,[1] D. H. Zhang,[43] G. Y. Zhang,[19] H. Zhang,[71] H. C. Zhang,[1,58,63] H. H. Zhang,[59] H. H. Zhang,[34] H. Q. Zhang,[1,58,63] H. Y. Zhang,[1,58] J. Zhang,[80] J. Zhang,[59] J. J. Zhang,[52] J. L. Zhang,[20] J. Q. Zhang,[41] J. W. Zhang,[1,58,63] J. X. Zhang,[38,j,k] J. Y. Zhang,[1] J. Z. Zhang,[1,63] Jianyu Zhang,[63] L. M. Zhang,[61] Lei Zhang,[42] P. Zhang,[1,63] Q. Y. Zhang,[39,80] R. Y. Zhang,[38,j,k] Shuihan Zhang,[1,63] Shulei Zhang,[25,h] X. D. Zhang,[45] X. M. Zhang,[1] X. Y. Zhang,[50] Y. Zhang,[72] Y. T. Zhang,[80] Y. H. Zhang,[1,58] Y. M. Zhang,[39] Yan Zhang,[71,58] Yao Zhang,[1] Z. D. Zhang,[1] Z. H. Zhang,[1] Z. L. Zhang,[34] Z. Y. Zhang,[76] Z. Y. Zhang,[43] G. Zhao,[1] J. Y. Zhao,[1,63] J. Z. Zhao,[1,58] Lei Zhao,[71,58] Ling Zhao,[1] M. G. Zhao,[43] R. P. Zhao,[63] S. J. Zhao,[80] Y. B. Zhao,[1,58] Y. X. Zhao,[31,63] Z. G. Zhao,[71,58] A. Zhemchugov,[36,a] B. Zheng,[72] J. P. Zheng,[1,58] W. J. Zheng,[1,63] Y. H. Zheng,[63] B. Zhong,[41] X. Zhong,[59] H. Zhou,[50] J. Y. Zhou,[34] L. P. Zhou,[1,63] X. Zhou,[76] X. K. Zhou,[6] X. R. Zhou,[71,58] X. Y. Zhou,[39] Y. Z. Zhou,[12,f] J. Zhu,[43] K. Zhu,[1] K. J. Zhu,[1,58,63] L. Zhu,[34] L. X. Zhu,[63] S. H. Zhu,[70] S. Q. Zhu,[42] T. J. Zhu,[12,f] W. J. Zhu,[12,f] Y. C. Zhu,[71,58] Z. A. Zhu,[1,63] J. H. Zou,[1] and J. Zu[71,58]

(BESIII Collaboration)

[1]*Institute of High Energy Physics, Beijing 100049, People's Republic of China*
[2]*Beihang University, Beijing 100191, People's Republic of China*
[3]*Bochum Ruhr-University, D-44780 Bochum, Germany*
[4]*Budker Institute of Nuclear Physics SB RAS (BINP), Novosibirsk 630090, Russia*
[5]*Carnegie Mellon University, Pittsburgh, Pennsylvania 15213, USA*
[6]*Central China Normal University, Wuhan 430079, People's Republic of China*
[7]*Central South University, Changsha 410083, People's Republic of China*
[8]*China Center of Advanced Science and Technology, Beijing 100190, People's Republic of China*
[9]*China University of Geosciences, Wuhan 430074, People's Republic of China*
[10]*Chung-Ang University, Seoul, 06974, Republic of Korea*
[11]*COMSATS University Islamabad, Lahore Campus, Defence Road,*
Off Raiwind Road, 54000 Lahore, Pakistan
[12]*Fudan University, Shanghai 200433, People's Republic of China*
[13]*GSI Helmholtzcentre for Heavy Ion Research GmbH, D-64291 Darmstadt, Germany*
[14]*Guangxi Normal University, Guilin 541004, People's Republic of China*
[15]*Guangxi University, Nanning 530004, People's Republic of China*
[16]*Hangzhou Normal University, Hangzhou 310036, People's Republic of China*
[17]*Hebei University, Baoding 071002, People's Republic of China*
[18]*Helmholtz Institute Mainz, Staudinger Weg 18, D-55099 Mainz, Germany*
[19]*Henan Normal University, Xinxiang 453007, People's Republic of China*
[20]*Henan University, Kaifeng 475004, People's Republic of China*

[21]Henan University of Science and Technology, Luoyang 471003, People's Republic of China
[22]Henan University of Technology, Zhengzhou 450001, People's Republic of China
[23]Huangshan College, Huangshan 245000, People's Republic of China
[24]Hunan Normal University, Changsha 410081, People's Republic of China
[25]Hunan University, Changsha 410082, People's Republic of China
[26]Indian Institute of Technology Madras, Chennai 600036, India
[27]Indiana University, Bloomington, Indiana 47405, USA
[28a]INFN Laboratori Nazionali di Frascati, I-00044 Frascati, Italy
[28b]INFN Sezione di Perugia, I-06100 Perugia, Italy
[28c]University of Perugia, I-06100 Perugia, Italy
[29a]INFN Sezione di Ferrara, I-44122 Ferrara, Italy
[29b]University of Ferrara, I-44122 Ferrara, Italy
[30]Inner Mongolia University, Hohhot 010021, People's Republic of China
[31]Institute of Modern Physics, Lanzhou 730000, People's Republic of China
[32]Institute of Physics and Technology, Peace Avenue 54B, Ulaanbaatar 13330, Mongolia
[33]Instituto de Alta Investigación, Universidad de Tarapacá, Casilla 7D, Arica 1000000, Chile
[34]Jilin University, Changchun 130012, People's Republic of China
[35]Johannes Gutenberg University of Mainz, Johann-Joachim-Becher-Weg 45, D-55099 Mainz, Germany
[36]Joint Institute for Nuclear Research, 141980 Dubna, Moscow region, Russia
[37]Justus-Liebig-Universitaet Giessen, II. Physikalisches Institut,
Heinrich-Buff-Ring 16, D-35392 Giessen, Germany
[38]Lanzhou University, Lanzhou 730000, People's Republic of China
[39]Liaoning Normal University, Dalian 116029, People's Republic of China
[40]Liaoning University, Shenyang 110036, People's Republic of China
[41]Nanjing Normal University, Nanjing 210023, People's Republic of China
[42]Nanjing University, Nanjing 210093, People's Republic of China
[43]Nankai University, Tianjin 300071, People's Republic of China
[44]National Centre for Nuclear Research, Warsaw 02-093, Poland
[45]North China Electric Power University, Beijing 102206, People's Republic of China
[46]Peking University, Beijing 100871, People's Republic of China
[47]Qufu Normal University, Qufu 273165, People's Republic of China
[48]Renmin University of China, Beijing 100872, People's Republic of China
[49]Shandong Normal University, Jinan 250014, People's Republic of China
[50]Shandong University, Jinan 250100, People's Republic of China
[51]Shanghai Jiao Tong University, Shanghai 200240, People's Republic of China
[52]Shanxi Normal University, Linfen 041004, People's Republic of China
[53]Shanxi University, Taiyuan 030006, People's Republic of China
[54]Sichuan University, Chengdu 610064, People's Republic of China
[55]Soochow University, Suzhou 215006, People's Republic of China
[56]South China Normal University, Guangzhou 510006, People's Republic of China
[57]Southeast University, Nanjing 211100, People's Republic of China
[58]State Key Laboratory of Particle Detection and Electronics,
Beijing 100049, Hefei 230026, People's Republic of China
[59]Sun Yat-Sen University, Guangzhou 510275, People's Republic of China
[60]Suranaree University of Technology, University Avenue 111, Nakhon Ratchasima 30000, Thailand
[61]Tsinghua University, Beijing 100084, People's Republic of China
[62a]Turkish Accelerator Center Particle Factory Group, Istinye University, 34010, Istanbul, Turkey
[62b]Near East University, Nicosia, North Cyprus, 99138, Mersin 10, Turkey
[63]University of Chinese Academy of Sciences, Beijing 100049, People's Republic of China
[64]University of Groningen, NL-9747 AA Groningen, The Netherlands
[65]University of Hawaii, Honolulu, Hawaii 96822, USA
[66]University of Jinan, Jinan 250022, People's Republic of China
[67]University of Manchester, Oxford Road, Manchester M13 9PL, United Kingdom
[68]University of Muenster, Wilhelm-Klemm-Strasse 9, 48149 Muenster, Germany
[69]University of Oxford, Keble Road, Oxford OX13RH, United Kingdom
[70]University of Science and Technology Liaoning, Anshan 114051, People's Republic of China
[71]University of Science and Technology of China, Hefei 230026, People's Republic of China
[72]University of South China, Hengyang 421001, People's Republic of China
[73]University of the Punjab, Lahore-54590, Pakistan
[74a]University of Turin and INFN, University of Turin, I-10125 Turin, Italy

[74b]*University of Eastern Piedmont, I-15121 Alessandria, Italy*
[74c]*INFN, I-10125, Turin, Italy*
[75]*Uppsala University, Box 516, SE-75120 Uppsala, Sweden*
[76]*Wuhan University, Wuhan 430072, People's Republic of China*
[77]*Yantai University, Yantai 264005, People's Republic of China*
[78]*Yunnan University, Kunming 650500, People's Republic of China*
[79]*Zhejiang University, Hangzhou 310027, People's Republic of China*
[80]*Zhengzhou University, Zhengzhou 450001, People's Republic of China*

[a]Also at the Moscow Institute of Physics and Technology, Moscow 141700, Russia.

[b]Also at the Novosibirsk State University, Novosibirsk 630090, Russia.

[c]Also at the NRC "Kurchatov Institute", PNPI, 188300 Gatchina, Russia.

[d]Also at Goethe University Frankfurt, 60323 Frankfurt am Main, Germany.

[e]Also at Key Laboratory for Particle Physics, Astrophysics and Cosmology, Ministry of Education; Shanghai Key Laboratory for Particle Physics and Cosmology; Institute of Nuclear and Particle Physics, Shanghai 200240, People's Republic of China.

[f]Also at Key Laboratory of Nuclear Physics and Ion-beam Application (MOE) and Institute of Modern Physics, Fudan University, Shanghai 200443, People's Republic of China.

[g]Also at State Key Laboratory of Nuclear Physics and Technology, Peking University, Beijing 100871, People's Republic of China.

[h]Also at School of Physics and Electronics, Hunan University, Changsha 410082, China.

[i]Also at Guangdong Provincial Key Laboratory of Nuclear Science, Institute of Quantum Matter, South China Normal University, Guangzhou 510006, China.

[j]Also at MOE Frontiers Science Center for Rare Isotopes, Lanzhou University, Lanzhou 730000, People's Republic of China.

[k]Also at Lanzhou Center for Theoretical Physics, Lanzhou University, Lanzhou 730000, People's Republic of China.

[l]Also at the Department of Mathematical Sciences, IBA, Karachi 75270, Pakistan.

[m]Also at Ecole Polytechnique Federale de Lausanne (EPFL), CH-1015 Lausanne, Switzerland.